Spontaneous Self-Assembly of Fully Protected Ester 1:1 [α/α- N α -Bn-hydrazino] Pseudodipeptides into a Twisted Parallel β-Sheet in the Crystal State

Eugénie Romero, Ralph-Olivier Moussodia, Alexandre Kriznik, Emmanuel Wenger, Samir Acherar, Brigitte Jamart-Gregoire

Spontaneous self-assembly of fully protected ester 1:1 [α/α-N^{α}-Bn-hydrazino] pseudodipeptides into a twisted parallel β-sheet in the crystal state

Eugénie Romero,[†] Ralph-Olivier Moussodia,[†] Alexandre Kriznik,[‡] Emmanuel Wenger,[§] Samir Acherar,*[,†] and Brigitte Jamart-Grégoire*[,†]

[†] Laboratoire de Chimie Physique Macromoléculaire (LCPM), Université de Lorraine-CNRS, UMR 7375, 1 rue Grandville, BP 20451, 54001 Nancy cedex, France

[‡] Ingénierie Moléculaire et Physiopathologie Articulaire (IMoPA Université de Lorraine – CNRS, UMR 7365), & Service Commun de Biophysique Interactions Moléculaires, Université de Lorraine, Biopôle de l'Université de Lorraine, Campus Biologie Santé – Faculté de Médecine, 9 Avenue de la Forêt de Haye, CS 50184, 54505 Vandœuvre-lès-Nancy, France

[§]Laboratoire de Cristallographie, Résonance Magnétique et Modélisations (CRM2), Université de Lorraine-CNRS, UMR 7036, Faculté des Sciences et Technologies, BP 70239, Boulevard des Aiguillettes, 54506 Vandœuvre-lès-Nancy cedex, France

Samir.Acherar@univ-lorraine.fr and Brigitte.Jamart@univ-lorraine.fr

Keywords: Self-Assembly, Twisted parallel β-sheet, Hydrazinopeptide, IR, NMR, Microcrystalline CD

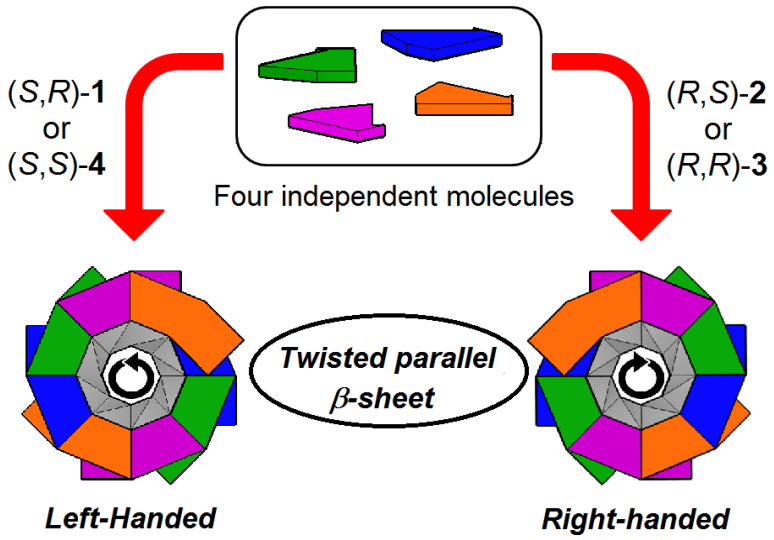

ABSTRACT

Previous studies have demonstrated that amidic α/β-pseudodipeptides, 1:1 [α/α-N^{α}-Bn-hydrazino], have the ability to fold *via* a succession of γ-turn (C_7 pseudocycle) and hydrazinoturn in $CDCl_3$ solution, their amide terminals enabling the formation of an intramolecular H-bond network. Despite their lack of a primary amide terminals allowing the formation of the hydrazinoturn, their ester counterparts **1**-**4** were proven to self-assemble into C_6 and C_7 pseudocycles by intramolecular H-bonds in solution state, and into an uncommon twisted parallel β-sheet through intermolecular H-bonding in the crystal state to form a supramolecular helix with eight molecules needed to complete a full 360° rotation. Such self-organization (with eight molecules) has been only observed in specific α/α-pseudodipeptide, depsipeptide (Boc-Leu-Lac-OEt). Relying on IR absorption, NMR, X-ray diffraction and CD analyses, the aim of this study was to demonstrate that stereoisomers of esters 1:1 [α/α-N^{α}-Bn-hydrazino] pseudodipeptide **1**-**4** are not only able to self-assemble into this β-helical structure. Their carbon's chirality will also influence the left- or right-handed twist without changing the pitch of the formed helix.

INTRODUCTION

Self-assembly consists in the spontaneous association of disordered individual entities into a well-defined arrangement. This process confers to these entities properties that they do not possess when taken individually. The spontaneous nature of the process is highlighted by the fact that this occurs without energetic input from an outside source, through the favorable formation of an H-bond network. Due to the weak nature of the interactions at play, upon external perturbation, such as changes in concentration, these assemblies can be reversed.

Many crucial biological functions rely on the ability of peptides to display particular folding/self-assembly patterns or secondary structures, called helices, turns and *β*-sheet, which occur through the formation of H-bonds established between *α*-amino acid backbone atoms. Among the various secondary structures, the *β*-sheet family, also called *β*-pleated sheet (Figure 1), is the less well studied for small-molecule structures. Their relative lack of study, compared to that of *α*-helices, can be considered quite surprising since the formation of supramolecular *β*-sheet architectures is at the basis of various neurodegenerative diseases such as Alzheimer's,[1] Huntington's,[2] prion protein[3] and other related diseases.[4]

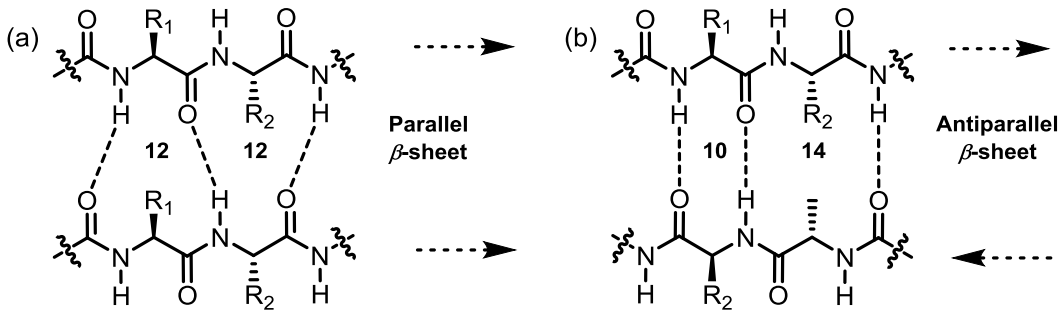

FIGURE 1. Hydrogen bond patterns in *β*-sheets: (a) parallel *β*-sheet (C_{12}pseudocycles) and (b) antiparallel *β*-sheet (C_{14} and C_{10}pseudocycles)

The use of peptides in biological applications such as drug delivery is severely hampered by their inherent propensity to rapid degradation through proteolysis. As an alternative, biologically active pseudopeptides, *i.e.* peptides with modified backbones, have emerged due to their potential resistance to peptidases and proteases and their ability to adopt well-defined secondary structures similar to their corresponding peptide analogs. Pseudopeptides have initially encompassed polyamides composed of amino acids other than α-amino acids such as β-peptides (Figure 2). The latter are the most widely investigated pseudopeptides, and have been extensively studied by Gellman and Seebach.[6,7] Indeed, they have been proven to not only be structured as their α-peptide analogues but to display stability against proteases and peptidases.[8]

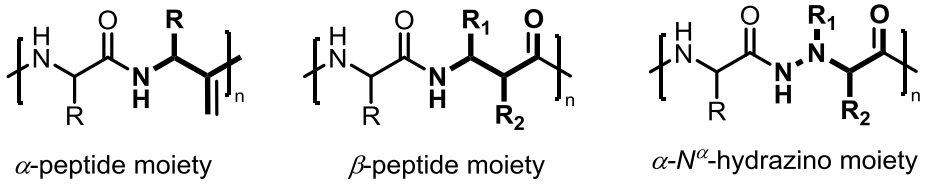

FIGURE 2. The backbones of α-peptide, β-peptide, and α-N^{α}-hydrazino moieties.

These pioneering studies have paved the way to the intensive studies of linear and cyclic β-peptides,[6,7,8] hybrid pseudopeptides consisting of α/β-, α/γ-, β/γ-amino acids,[9] together with the less common studies of β/δ- and γ/δ-pseudopeptides.[10] The use of heterogenous backbones in pseudopeptidic designs was indeed justified by studies in the 2000's indicating the relevance of the introduction of a β-amino acid in a peptide to both increase the proteolysis stability[11] and induce a preorganization that could lead to new folding possibilities.[9c]

Extending the β-peptide concept has given birth to bis-nitrogenated compounds in which the C^{β} has been replaced by a nitrogen atom, leading to the new family of "hydrazinopeptides".[12] Previous studies in our laboratory have illustrated the ability of mixed amidic 1:1 [α/α-N^{α}-hydrazino]mers to fold into a hydrazinoturn (Figure 3). This specific feature consists in the

formation of a bifurcated hydrogen bond through C_5 and C_8pseudocycles, involving the lone pair of the N^{α}-atom, together with a γ-turn (C_7pseudocycle). Interestingly, the same intramolecular H-bond network is formed regardless of the chirality.[13]

Subsequent studies of their macrocyclic counterparts have shown their ability to self-assemble into nanotubes *via* the formation of an intermolecular H-bond network.[14]

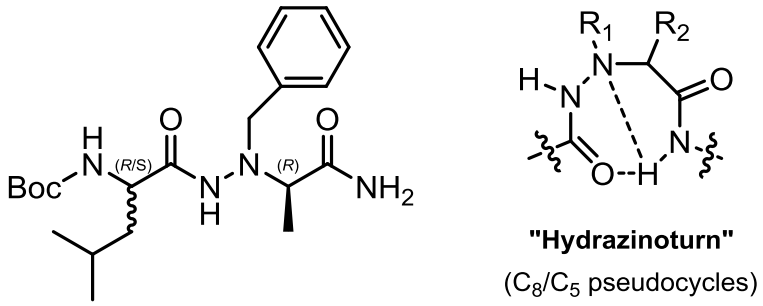

FIGURE 3. Self-organization of amidic 1:1[α/α-N^{α}-Bn-hydrazino] pseudodipeptides through the "hydrazinoturn". C_5 is Ni+1-H···Ni and C_8 is Ni+1-H···Oi-1=C.

Such versatile self-structuration emphasized the particular role of the hydrazino link within this pseudopeptide series. These results led us to envision the possibility of gaining access to various secondary structures by wisely manipulating this particular backbone.

As currently employed to evaluate the role of the amide bond in protein folding, we have replaced the amide terminals by an ester through "amide-to-ester mutagenesis",[15] thereby preventing our newly formed ester 1:1 [α/α-N^{α}-Bn-hydrazino] pseudodipeptide from folding into a hydrazinoturn. We propose that this backbone modification should open the door to new "intermolecular" self-assemblies promoted by the intrinsic preorganization of the hydrazinopeptides.[16]

We thus undertook the synthesis of ester 1:1 [α/α-N^{α}-Bn-hydrazino] pseudodipeptides **1**-**4**. Because of the influence of the chirality on the supramolecular edifice, we decided to supplement this work with a comprehensive study of the chirality effect by synthesizing and

characterizing four stereoisomers **1**-**4**, as shown in Figure 4. It is important to note that compounds **1-4** possess an sp^3 nitrogen atom (N^{α}-atom) which can be regarded as an extra chiral center with a non-fixed configuration. Comparisons of (*S*,*R*)-**1** and (*R*,*S*)-**2**, or (*R*,*R*)-**3** and (*S*,*S*)-**4** enable us to verify if reversing the chirality of carbons also leads to the chirality inversion of the N^{α}-atom.

Herein, we resort to X-ray crystallography and microcrystalline CD analysis together with NMR and IR absorption analyses to unveil not only the first spontaneous self-assembly in a twisted β-sheet observed within 1:1 [α/α-N^{α}-hydrazino] pseudodipeptides **1**-**4**, but also the chirality effect on the left- or right-handed twist of the formed supramolecular helix.

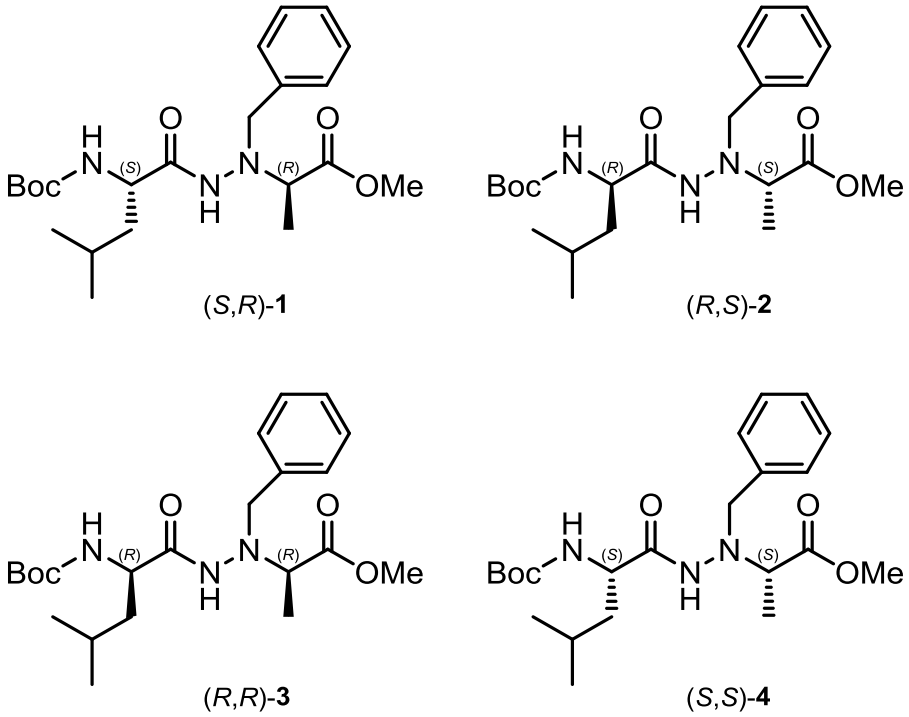

FIGURE 4. Chemical structures of the stereoisomers of ester 1:1[α/α-N^{α}-Bn-hydrazino] pseudodipeptides **1**-**4**

RESULTS AND DISCUSSION

Studies of the self-assembly in solution state by ^{1}H NMR experiments and FTIR spectroscopy

Ester [α/α-N^{α}-hydrazino] pseudodipeptides **1**-**4** were synthesized according to our previously described procedure.[13]

In a first step, the conformation of the stereoisomers **1**-**4** in solution state was studied through ^{1}H NMR and FTIR techniques and, given the fact that each of these provides the same results (see Supporting Information pp S2 to S9), only compound (*S*,*R*)-**1** is described below (Figure 5).

The study of the concentration dependence of the chemical shift of the carbamidic (NHBoc) and hydrazidic NH protons in $CDCl_3$ solution, from 10^{-4} to 10^{-1} M, was performed by ^{1}H NMR (Figure 5a) and showed a complete lack of sensibility correlation. The chemical shift of these NH protons remained unchanged over this concentration range with values of approximately 4.8 and 8.0 ppm, respectively, which allows us to conclude that no intermolecular H-bonding occurs in the compound (*S*,*R*)-**1**. On the basis of small model compounds described in one of our earlier studies,[17f] we established that the chemical shifts of non-bonded carbamic and hydrazidic NH protons are estimated to be roughly 4.7 and 6.5 ppm, respectively, which enables us to assume that the carbamic NH proton is non-bonded, contrary to the hydrazidic NH proton.

To validate these assumptions, we also worked in a mixture of $CDCl_3$/DMSO-d_6 (c = 10^{-2} M, from 0 up to 10%, Figure 5b) with the aim of assessing NH protons involved in an intramolecular H-bond. Solvents with H-bond acceptor atoms, such as DMSO-d_6, are able to form intermolecular H-bonds producing a downfield shift which is less significant when the H-atom participates in an intramolecular H-bond. This type of experiment has been proven to be efficient in evaluating the H-bond strength.[17] As shown in Figure 5b, the chemical shift of

the hydrazidic NH proton is independent of the amount of DMSO, which means that it is involved in an intramolecular H-bond, unlike the carbamidic NH proton (NHBoc) which is non-bonded due to its sensitivity to DMSO.

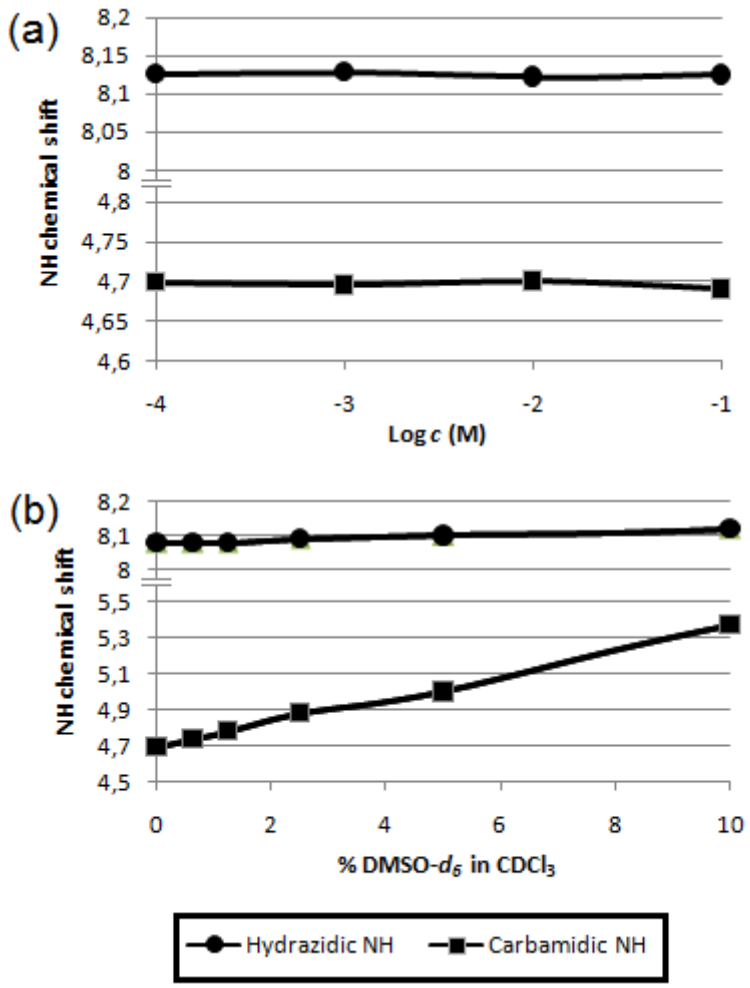

FIGURE 5. (a) Concentration-dependence in $CDCl_3$ (from 10^{-1} to 10^{-4} M) and (b) solvent dependence as determined by ^1H NMR (300 MHz) in mixed $CDCl_3$/DMSO-d_6 (c = 10^{-2} M) of NH chemical shifts of **1**

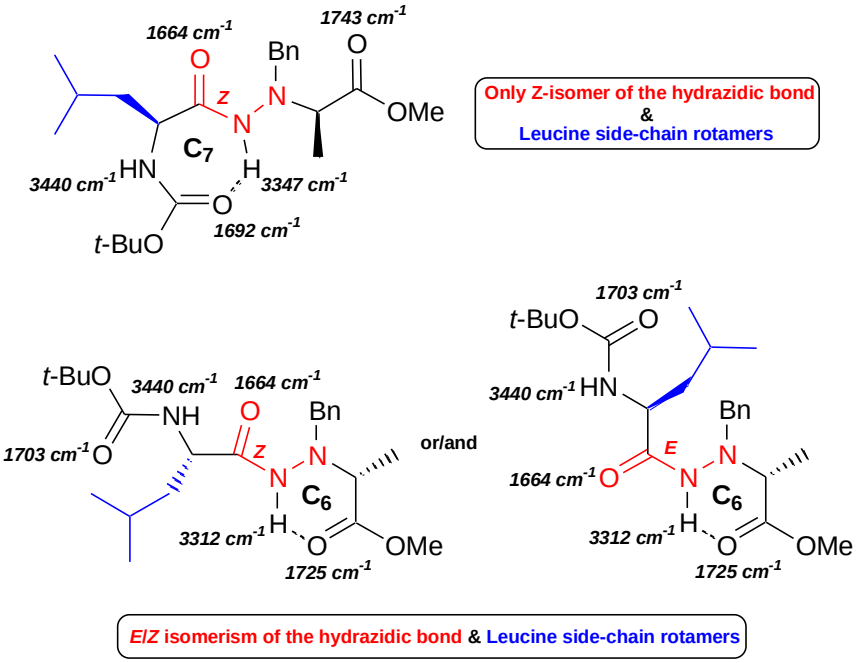

FIGURE 6. Conformations for compound **1** in $CDCl_3$ solution

Careful inspection of the ^{13}C NMR spectrum of compound (*S*,*R*)-**1** (see Supporting Information pp S2 to S5), revealed an additional minor set of signals, demonstrating the presence of a several conformations in CDCl3 solution. These various conformations were due to the possible presence of E/Z isomerism of the hydrazidic bond and leucine side-clain rotamers. At this point, two possible conformations (C_6 and C_7 pseudocycles), involving the hydrazidic NH proton, were envisioned (Figure 6).

To complement these NMR results, FTIR absorption spectroscopic studies were conducted in $CDCl_3$ at a concentration where intermolecular contacts have been proved nonexistent (c = 10^{-2} M). FTIR spectroscopy is an efficient method to detect several conformers in solution by given differentiable N-H and C=O signals for each conformer.[18]

Figure 7 presents the IR spectra of N-H and C=O stretching regions of compound (*S*,*R*)-**1** (three and five bands, respectively). For the N-H stretching region, the first band at 3440 cm^{-1}, located in the free N-H domain (> 3400 cm^{-1}),[16,18] corresponds to the non-bonded NHBoc and the two other bands at 3347 and 3312 cm^{-1} are assigned to the bonded hydrazidic NH which is

involved in both conformations described above (Figure 6). Among the 5 bands observed in the C=O domain, 4 bands, (1743/1725 cm^{-1} and 1703/1692 cm^{-1}) are assigned to the ester and carbamidic CO (free/bonded) respectively and the last one located at 1664 cm^{-1} to the free hydrazidic CO, which is not involved in any intramolecular H-bond. These FTIR results are an endorsement of our hypothesis that compound (*S*,*R*)-**1** adopts both C_6 and C_7 conformations in $CDCl_3$ solution (Figure 6).

The maintainence of this conformational equilibrium at high concentration (c =1 M, $CDCl_3$) was demonstrated by obtaining the same kind of FTIR analysis. It is noteworthy also that these analyses have been carried out in other solvents (c = 10^{-2} M) such as toluene and methanol (see Supporting Information pp S10 and S11) and have led to the same self-organization.

To investigate and confirm the conformational equilibrium adopted by compounds **1**-**4** in solution, we undertook their analyses in the crystal state.

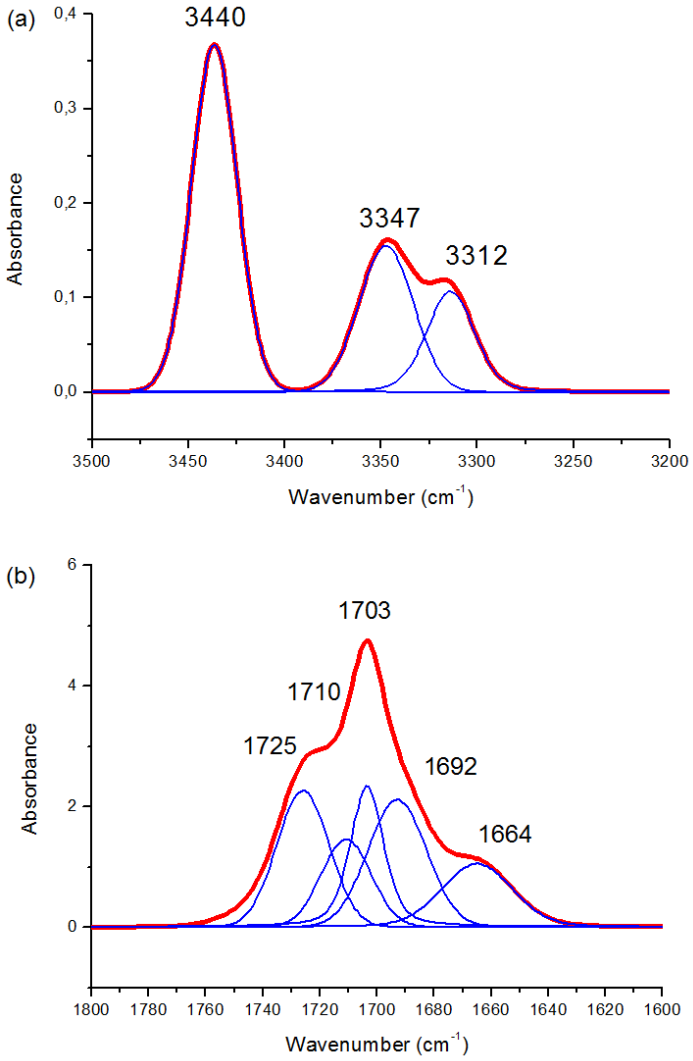

FIGURE 7. IR spectra (in red) and deconvoluted IR spectra (in blue) of (a) N-H and (b) C=O stretching regions in $CDCl_3$ ($c = 10^{-2}$ M) of **1**

Studies of the self-assembly of 1-4 in the crystal state by X-ray diffraction

Crystals of compounds **1-4** were grown by slow evaporation from a dichloromethane/petroleum ether solution and crystallized in the space group $P2_12_12_1$ (see Supporting Information pp S12 to S23 for more details). Crystallographic data and structure refinement parameters are reported in CIF format with CCDC references 1447540 to 1447543 (a copy of CIF formats are available in Supporting Information). The crystal structure

determination of (*S*,*R*)-**1** and (*R*,*S*)-**2** was obtained from low-resolution X-ray diffraction data collected at 100K (R-factor values of 6.92 and 9.56% respectively). Regarding compounds (*R*,*R*)-**3** and(*S*,*S*)-**4**, poor X-ray diffraction data were collected (R-factor values of 17.04 and 12.14% respectively). Consequently, their crystal structures are less resolved but are still sufficient to confirm the packing and the folding.

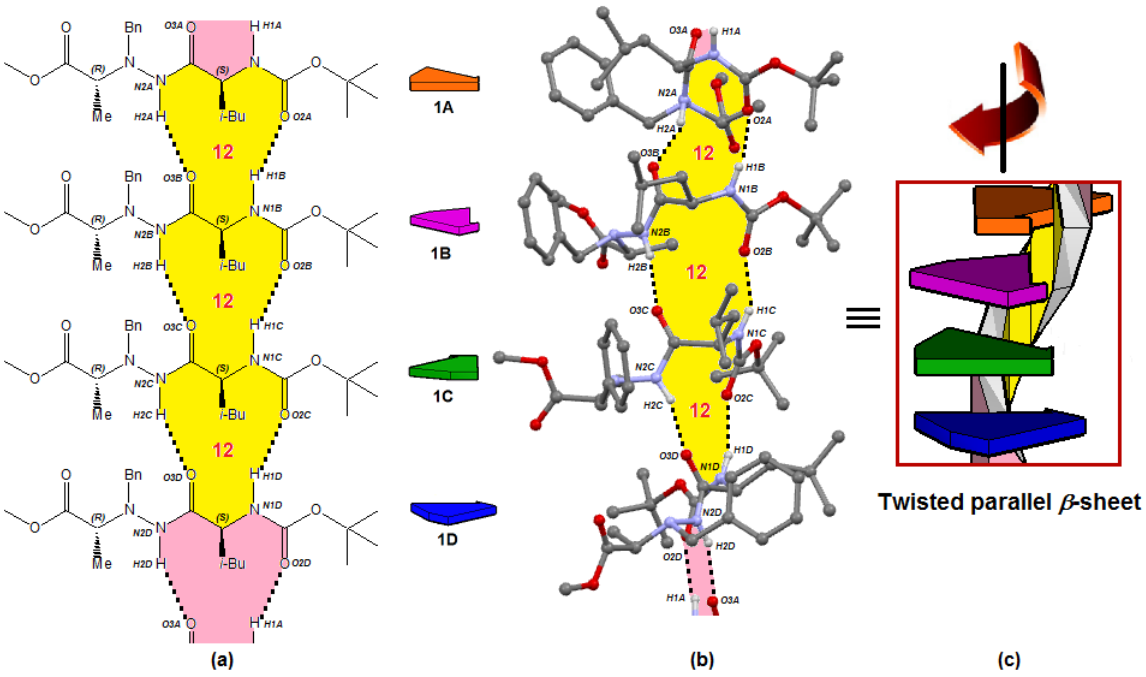

FIGURE 8. (a) Hydrogen bond patterns between four independent molecules (1A-1D), (b) 12-membered hydrogen-bonded rings and (c) cartoon representation of the twisted parallel *β*-sheet for **1**

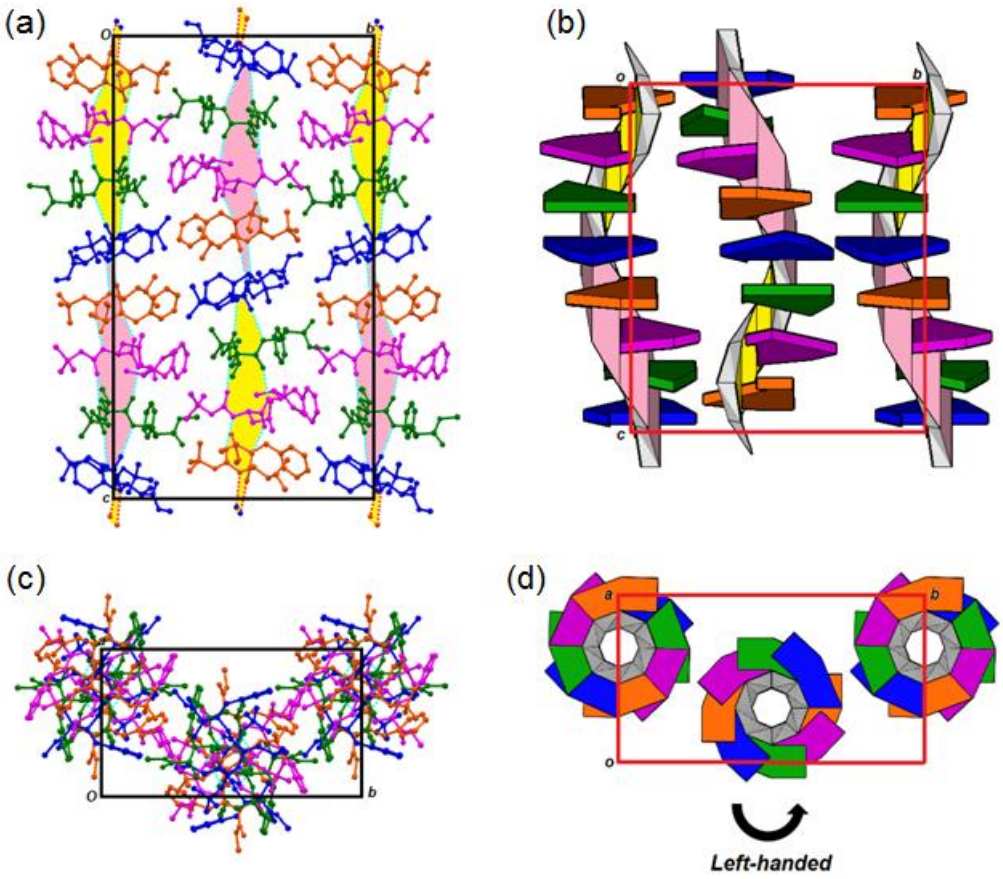

FIGURE 9. (a,c) Molecular packing and (b,d) cartoon representation of the twisted parallel *β*-sheet of **1** viewed along the *a* and *c* axis respectively

The X-ray structure of the heterochiral ester (*S*,*R*)-**1** corresponds to sixteen molecules in the unit cell (four molecules 1A-1D in the asymmetric unit) and the N^{α}-atom has a pyramidal conformation with (*S*)-configuration (Figures 8 and 9).

The four independent molecules 1A-1D stacked one atop the other form a tetramer block and two of these can interact together to provide an octamer block. This tetrameric/octameric association is maintained through an intermolecular H-bonding network between the carbamidic C=O and NH and the hydrazidic C=O and NH of each molecule 1A-1D, closing a 12-membered H-bonded pseudocycle with a distance $d_{(C=O\cdots H-N)}$ of 1.98 to 2.16 Å (Figures 8, 9 and Table S2 in Supporting Information) demonstratinf a parallel *β*-sheet arrangement as indicated in Figure 1.

The data collected from the crystal analysis of the intermolecular packing clearly show no intramolecular bonds in the crystal lattice, as evidenced by the high nuclear distances. The "*β*-strand" molecules stack up on top of each other into a parallel fashion through intermolecular H-bonds. However, the most interesting feature of this self-assembly is the presence of a twist that shapes a left-handed helical supramolecular structure. The formation of a helical structure will be referred to as a twisted *β*-sheet. It is noteworthy that the formed helix requires eight molecules to complete a full 360° rotation with a pitch of 38.20 Å. In the CCDC database, there are various examples of acyclic dipeptides with parallel *β*-sheet structures [19] (flat tapes or twisted with different numbers of molecules per turn) but only one parallel twisted *β*-sheet was observed with eight molecules per turn (depsidipeptideBoc-Leu-Lac-OEt).[20]

By taking a close look at the torsion angle values (*ω*, *ϕ* and *ψ*) of the Leu residue, responsible for the left-handed helical supramolecular structure, we have found that these values are closely related to the left-handed type-II poly(L-Pro)$_n$ conformation (Table 1) [21] but the supramolecular helix is approximately four times more elongated than type II poly(L-Pro)$_n$ helix by comparing their helical pitch (Table 1).

TABLE 1. Selected parameters characterizing the left-handed helical supramolecular structure in **1** and the left-handed type-II poly(L-Pro)$_n$ helix.

	Supramolecular helix in **1**	type-II poly(L-Pro)$_n$ helix
ω (°)	+172 to +180	+180
ϕ (°)	–81 to –70	– 80
ψ (°)	+115 to +124	+150
n	8[a]	3[b]
Pitch (Å)	38.20	9.3

[a]Number of residues (L-Pro) per helical turn for the type-II poly(L-Pro)$_n$ helix

[b]Number of molecules per helical turn for the supramolecular helix in **1**

X-ray analysis of compound (*R*,*S*)-**2** showed that changing the α-carbon chirality of both the α-amino acid and the α-N^{α}-Bn-hydrazino acid residues in our pseudodipeptide backbone reverses the chirality of the N^{α}-atom. As a result, the corresponding heterochiral (*R*,*S*)-**2** is the enantiomer of (*S*,*R*)-**1** and logically leads to a reverse turn of the β-helical structure, *i.e.* compound (*R*,*S*)-**2** adopts a right-handed twist with the same helical pitch (38.19 Å, Figure 10).

The question as to which chiral center is responsible for the helicity then arose the answer is not obvious since it is known that an achiral pseudodipeptide (CCDC Refcode XEZDUC) is able to form a parallel twisted β-sheet self-assembly.[22] To study this question, we proceeded to synthesize and assess the crystal structures of homochiral (*R*,*R*)-**3** and (*S*,*S*)-**4** stereoisomers. The results were unambiguous and are presented in Table 2.

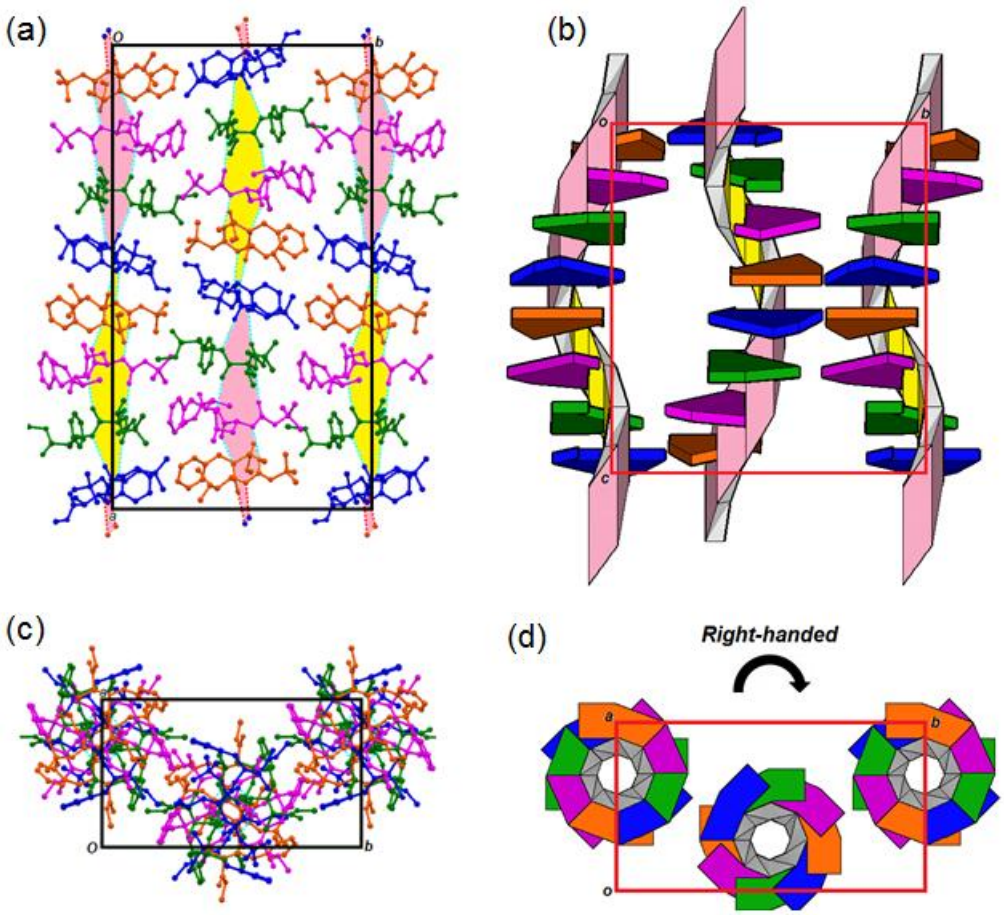

FIGURE 10. (a,c) Molecular packing and (b,d) cartoon representation of the twisted parallel *β*-sheet of **2** viewed along the *a* and *c* axis respectively

TABLE 2. Summary of the handedness of the helices adopted by **1-4** in the crystal state

Compound	Chirality of the N^{α}-atom	Twist direction of the helix	Pitch (Å)
*(S,R)-**1***	*S*	*Left-handed*	*38.20*
*(R,S)-**2***	*R*	*Right-handed*	*38.19*
*(R,R)-**3***	*R*	*Right-handed*	*38.17*
*(S,S)-**4***	*S*	*Left-handed*	*38.21*

The crystallographic analysis of homochiral compounds (*R*,*R*)-**3** and (*S*,*S*)-**4** (see Supporting Information pp S19 to S24) demonstrated the same kind of *β*-helical structures as those observed with homochiral compoundswitha left- and right-handed twist, respectively. The crystal structure of (*R*,*R*)-**3** corresponds to sixteen molecules in the unit cell (four molecules of 3A-3D in the asymmetric unit) with the N^{α}-atom having a pyramidal conformation with (*R*)-configuration as with the crystal structure of (*R*,*S*)-**2**. As previously, the chirality inversion of N^{α}-atom between (*R*,*R*)-**3** and (*S*,*S*)-**4** occurred, making them an enantiomeric couple, with a N^{α}-atom adopting the same configuration as the C^{α}-atom of the *α*-amino acid residue. Therefore, this alternating switch of the helicity, without changing the helical pitch, can undoubtedly be attributed to the *α*-carbon chirality of the *α*-amino acid residue by comparison of the crystal structures of stereoisomers **1**-**4**.

Indeed, a careful consideration of the intermolecular H-bond network points out that only one of the two asymmetric carbons present in the 1:1 [*α*/*α*-N^{α}-Bn-hydrazino] pseudodipeptide backbone, namely the *α*-amino acid C^{α}, is involved in the formation of the 12-membered H-bond pseudocycle responsible for the parallel *β*-sheet formation (Figure 9).

This seems to pinpoint the fact that a D-amino acid in the ester 1:1 [α/α-N^{α}-Bn-hydrazino] pseudodipeptide series will induce a right-handed twisted β-sheet, while its L-amino acid counterpart will lead to a left-handed helical structure.

Studies of the self-assembly of 1-4 in the crystal state by microcrystalline Circular Dichroism

The poor quality crystals of some compounds make single crystal X-ray diffraction somewhat difficult; however, a microcrystalline powder of these compounds is easily obtained. These powders can be used in the microcrystalline state in order to confirm X-ray predictions, that the direction of the β-helical structure is controlled by the α-carbon chirality of the α-amino acid residue.

In this context, CD spectroscopy has been widely used to investigate structural changes in non-racemic chiral organic molecules. While it is frequently performed in solution, solid-state CD analysis, through the microcrystalline technique, also represents a powerful tool that provides crucial specific supermolecular information.[23]

With the aim of optimizing results, microcrystals of **1-4** were suspended in Nujol oil (c = 25-50 mg.mL^{-1}), which is required to achieve a viscous suspension. Figure 11 depicts microcrystalline CD spectra of compounds **1-4** and it is worth mentioning that Nujol oil has no effect on the CD signal.

As illustrated in Figure 11, the shape of CD curves differs from those conventionally used for the determination of protein secondary structure (α-helix, β-sheet or random coil)[24] and provides a specific signal for both homochiral and heterochiral series. In each series, we

clearly observed an inversion of the CD signal, which confirms the presence of two pairs of enantiomers as well as the complete chirality control of the N^{α}-atom in the crystal state.

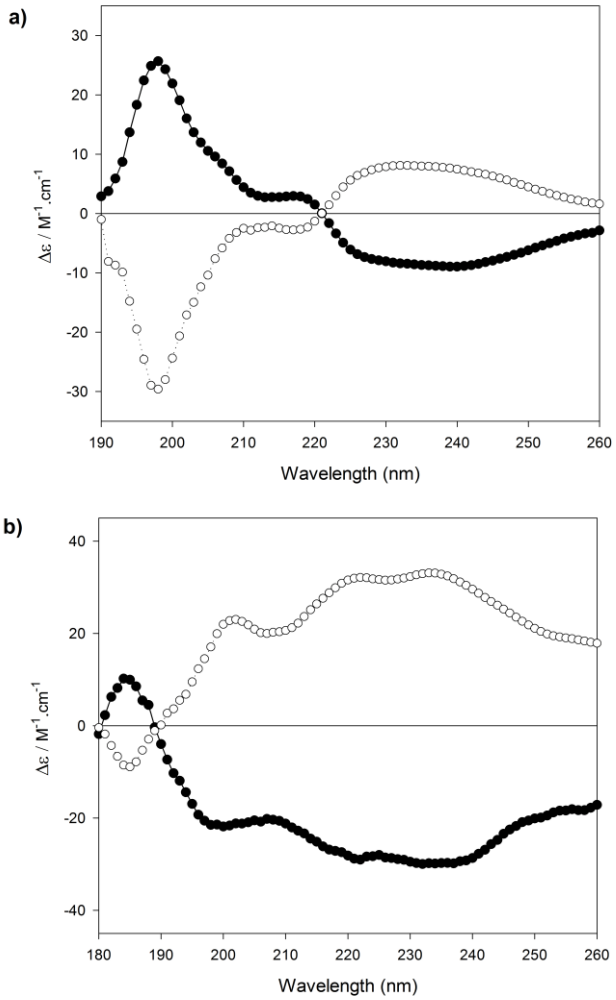

FIGURE 11. Microcrystalline normalized CD spectra of pseudodipeptides **1**-**4**, in Nujol mulls (*c* = 25-50 mg.mL^{-1}), in 0.01 cm quartz flat cells, at 293 K; Nujol blank was subtracted from the spectra: (a) Superimposition of homochiral compounds (*R*,*R*)-**3** and (*S*,*S*)-**4** CD spectra. (b) Superimposition of heterochiral compounds (*S*,*R*)-**1** and (*R*,*S*)-**2** CD spectra

In the homochiral series (Figure 11a), compound (*R*,*R*)-**3** presents, contrary to its enantiomer (*S*,*S*)-**4**, only one broad positive band centered at approximately 233 nm, and two negative bands estimated at 217 and 198 nm. It should also be noted that the CD signal intensities of

the heterochiral series are weak and were only recordable by using SRCD (synchrotron radiation CD).

By correlating the X-ray and CD results of (*R*,*R*)-**3** and (*S*,*S*)-**4**, we can conclude that the shape of the curves of (*R*,*R*)-**3** and (*S*,*S*)-**4** refer to right- and left-handed helical *β*-sheet structures, respectively.

To support these conclusions, compound **5** was synthesized and analyzed and compared to compound **6** previously described[13] (Figure 12). Pseudodipeptide **5**, an analogue of (*S*,*R*)-**1** and of (*R*,*R*)-**3** has a glycine residue instead of leucine, allows assessment of the chirality impact of the *α*-amino acid on the supramolecular self-assembly while compound **6**, a *C*-terminal amide analogue of (*S*,*R*)-**1**, allows assessment of whether the addition of a new hydrogen bond donor site may prevent a self-assembly into *β*-sheets due to the hydrazinoturn (an intramolecular bifurcated hydrogen bond) formation.

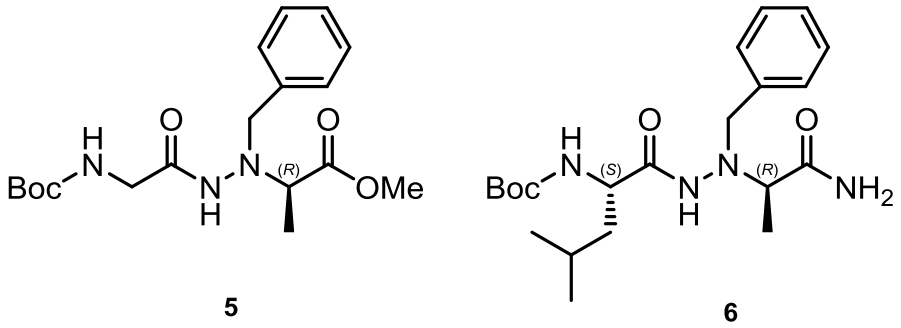

FIGURE 12. Chemical structure of pseudodipeptides **5**-**6**

Crystals of compounds **5** and **6** were grown by slow evaporation from a dichloromethane/ petroleum ether mixture, but once again, the poor quality crystals prevented us from performing the X-ray analysis. However, as noted earlier, the microcrystalline CD spectra of these compounds could be recorded on a CD spectrometer as for homochiral compounds (*R*,*R*)-**3** and (*S*,*S*)-**4** (Figure 13).

Concerning the CD signals of compounds **5** (Figure 13a) and **6** (Figure 13b), these bear strong resemblance to aryl benzyl sulfoxide compounds. In fact, only the CD signal arising from the benzyl part of **5** is detected with a particular negative maximum value at 230 nm.[25] This observation suggests that the presence of a new hydrogen bond donor site at the *C*-terminal position may prevent a supramolecular self-assembly into *β*-sheets possibly due to an intramolecular bifurcated hydrogen bond (called hydrazinoturn), as was previously demonstrated in the $CDCl_3$ solution state.[13]

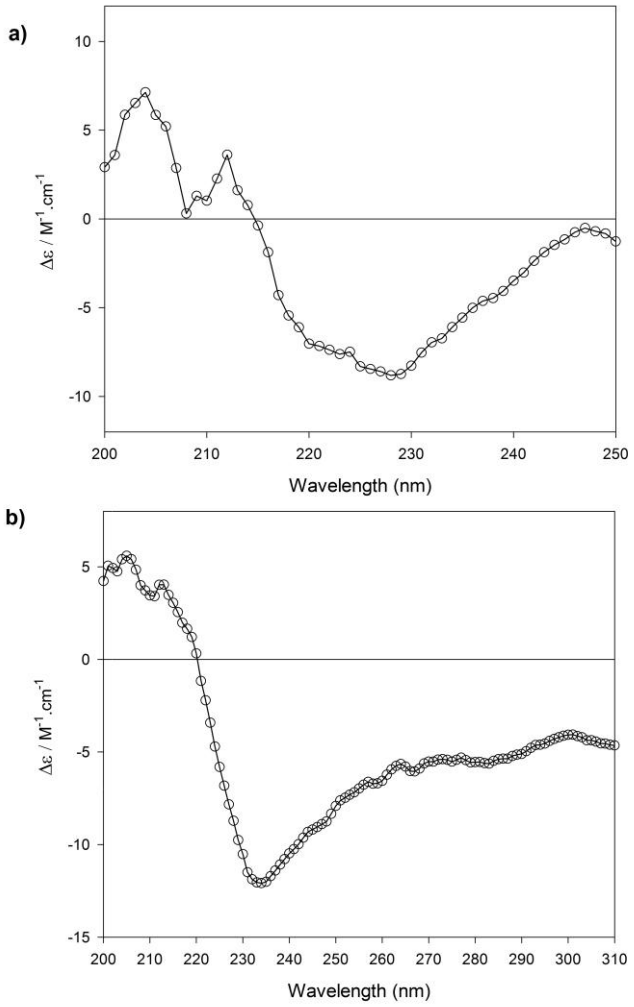

FIGURE 13. Microcrystalline normalized CD spectra of pseudodipeptides **5** (a) and **6** (b), in Nujol mulls (c = 50 $mg.mL^{-1}$), in 0.01 cm quartz flat cells, at 293 K; Nujol blank was subtracted from the spectra

CONCLUSION

In summary, we highlight in this work the formation of a twisted β-sheet supramolecular structure in the crystal state for fully protected 1:1 [α/α-N^{α}-Bn-hydrazino] pseudodipeptides **1**-**4** by using X-ray studies supplemented by CD studies of pseudodipeptides **1**-**6**. It has been shown that the N^{α} atom chirality is fixed and adopts the same configuration as the C^{α}-atom of the α-amino acid residue. Also, the switch of the helicity, without changing the helical pitch, was attributed to this same C^{α}-atom by comparing X-ray structures of stereoisomers **1**-**4**. Finally, this supramolecular β-helical structure is not maintained in the solution state, leaving in its place a conformational equilibrium between C_6 and C_7 pseudocycles.

The study of the morphology of pseudodipeptides **1**-**4** by SEM analyses in order to determine if these pseudodipeptides can generate any amyloid-like fibrils through β-sheet mediated self-assembly, which is a main cause of the neurodegenerative disease Alzheimer's, is currently in progress.

EXPERIMENTAL SECTION

NMR

All NMR spectra (1D and 2D) were recorded at 298K on a 300 MHz spectrometer with tetramethylsilane (TMS) as the internal standard. Chemical shifts (δ) are reported in ppm downfield from $CDCl_3$ (δ = 7.26 ppm) for ^{1}H NMR and relative to the central $CDCl_3$ resonance (δ = 77.0 ppm) for ^{13}C NMR spectroscopy.

^{13}C multiplicity data were obtained from JMOD experiments (C and CH_2 up, CH_3 and CH down).

For ^{1}H NMR spectroscopic data, the coupling constants (J) are given in Hz and the multiplicity is defined as: s for singlet; d for doublet; q for quartet; m for multiplet; br for broad, or combinations thereof.

Assignment of ^{1}H and ^{13}C NMR spectra were aided by COSY, ROESY, JMOD, HSQC and HMBC experiments.

For each compound, ^{1}H and ^{13}C NMR data indicated the presence of multiple conformations in $CDCl_3$ solution due in large part to the *E*/*Z* isomerism of the hydrazidic bond [26] and/or the possible rotamers of the leucine side chain.[27] Only the chemical shifts of the major conformations are given.

For the concentration dependence experiment in $CDCl_3$, the chemical shift of each NH proton was measured under four different concentrations (10^{-4}, 10^{-3}, 10^{-2} and 10^{-1} M).

For the solvent dependence experiment, the chemical shift of each NH proton was measured at a 10 mM concentration at various percentages of DMSO-d_6 in $CDCl_3$ (0, 0.625, 1.25, 2.5, 5 and 10%).

FTIR

Infrared spectra were recorded with an attenuated total reflectance Fourier transform infrared (FTIR) spectrophotometer equipped with Mid-IR source, KBr beamsplitter, and a liquid-nitrogen-cooled mid-band mercury cadmium telluride (LN-MCT Narrow) detector. Each spectrum was recorded over 256 scans at 298K and obtained in $CDCl_3$ (c = 10 mM) with a CaF_2 cell of 500 μm path length at a concentration of 10 mM. After subtraction of the solvent spectrum ($CDCl_3$).

The deconvolution method was used to resolve the overlapping bands in the NH and C=O stretching regions and the resulting deconvoluted spectra provided information about the conformational equilibrium occurring in the $CDCl_3$ solution. The deconvolution of N-H and C=O stretching region bands (3500-3200 cm^{-1} and 1800-1600 cm^{-1} respectively) was performed with the OPUS software package (version 6.5). Band positions were determined based on fixed number bands obtained from the second derivatives of the original spectra. These bands were automatically adjusted by the damped least-squares optimization algorithm developed by Levenberg-Marquardt. The obtained root mean square error (RMSE) was below 0.0009 for each spectrum.

Circular Dichroism

Microcrystalline CD spectra were recorded on a CD spectropolarimeter, scanned on the far-UV range, at 293K with 1 nm steps from 260 to 190 nm and averaged over 3 scans. Between each scan, a delay of 5 min was respected in order to detect any UV induced modification.[28] For each compound no spectra shape modification was noted. Crystals were crushed with a

mortar to obtain a very small granulation, and the microcrystals were then suspended in Nujol oil at a final concentration of 25 or 50 mg.mL-1. This preparation provided an optimum homogeneity of Nujol mull, allowing to avoid depolarization or scattering effects.[29] Absorbance was simultaneously registered and checked for any variation between isomers. Moreover, to demonstrate the absence of detectable artefactual signals,[30] several measurements were done with different angles by inverting engraved 0.01 cm pathlength cells by a 180° flip on the y-axis and 90° rotations on the z-axis. With these control conditions, all measurements remained unchanged, providing similar spectra. Absorbance levels, below 1.5 AU, between hetero then homo compounds, were superimposable with each other.

X-ray diffraction

Crystals of compounds **1**-**4** exhibited weak diffracting intensities. Their X-ray data were collected at 100K with a Rigaku Oxford Diffraction SuperNova diffractometer equipped with a copper microsource (λ = 1.54184 Å) and an Atlas CCD detector. Diffraction data were processed using CrysAlis PRO (Rigaku Oxford Diffraction, 2014). The structure was solved by direct methods with SIR2014.[31] The structure models refinements were conducted using a spherical atom model with ShelXle.[32] All X-ray data for each compound (**1**-**4**) are deposited in the CCDC database under access numbers: 1447540, 1447541, 1447542, and 1447543 respectively. Selected crystallographic data for **1**-**4** are provided in the Supporting Information.

HRMS

The ESI-HRMS analysis was conducted using a quadrupole-time-of-flight (QTOF) mass spectrometer equipped with an Apollo II ion funnel ESI Electrospray source (1 μL - 1 mL/min).

Synthesis

Compounds **1**-**6** were prepared according to reference 13.

Heterochiral pseudodipeptides Boc-[(L)-Leucine-*α*-N^{α}-benzyl-(D)-hydrazinoalanine]-OMe and Boc-[(D)-Leucine-*α*-N^{α}-benzyl-(L)-hydrazinoalanine]-OMe, (*S*,*R*)-1 and (*R*,*S*)-2. White powder. Characterization data: mp 112°C; ^{1}H NMR (300 MHz, $CDCl_3$, 10 mM) δ 0.89 (d, 6H, J = 6.3 Hz, 2 δCH_3Leu), 1.23-1.65 (m, 6H, βCH_3Ala, βCH_2Leu, γCH Leu), 1.47

(s, 9H, Boc), , 3.72-3.83 (m, 1H, αCH Ala), 3.78 (s, 3H, OCH_3), 3.88-4.13 (m, 3H, CH_2, N^{α}-Bn, αCH Leu), 4.77 (br s, NHBoc), 7.23-7.43 (m, 5H, Ar.), 7.98 (s, 1H, NH hydrazidic); ^{13}C NMR (75 MHz, $CDCl_3$) δ 16.3 (βCH_3Ala), 22.7 (2 δCH_3Leu), 24.6 (γCH Leu), 28.3 (3 CH_3, Boc), 41.2 (βCH_2Leu), 51.6 (O-CH_3), 52.3 (αCH Leu), 60.0 (αCH Ala), 60.1 (CH_2, N^{α}-Bn), 79.9 (C, Boc), 127.6 (CH, Ar.), 128.3 (2 CH, Ar.), 129.3 (2 CH, Ar.), 136.3 (C, Ar.), 155.3 (C=O, Boc), 171.1 (C=O, hydrazid), 174.6 (C=O, ester); HRMS (ESI) calculated for $C_{22}H_{35}N_3O_5$ $[M+H]^+$ *m/z* 422.2655, found 422.2649 and 422.2646.

Homochiral pseudodipeptides Boc-[(D)-Leucine-*α*-N^{α}-benzyl-(D)-hydrazinoalanine]-OMe and Boc-[(L)-Leucine-*α*-N^{α}-benzyl-(L)-hydrazinoalanine]-OMe, (*R*,*R*)-3 and (*S*,*S*)-4.White powder. Characterization data: mp 83°C; ^{1}H NMR (300 MHz, $CDCl_3$, 10 mM) δ 0.94 (d, 6H, J = 6.3 Hz, 2 δCH_3Leu), 1.34-1.56 (m, 6H, , βCH_3Ala, βCH_2Leu, γCH Leu), 1.43 (s, 9H, Boc), 3.68-3.79 (m, 1H, αCH Ala), 3.75 (s, 3H, OCH_3), 3.82-3.93 (m, 1H, αCH Leu), 3.96-4.08 (m, 2H, CH_2, N^{α}-Bn), 4.80 (br s, NHBoc), 7.23-7.39 (m, 5H, Ar.), 7.93 (s, 1H, NH hydrazidic); ^{13}C NMR (75 MHz, $CDCl_3$) δ 16.1 (βCH_3Ala), 22.6 (2 δCH_3Leu), 24.4 (γCH Leu), 28.3 (3 CH_3, Boc), 41.1 (βCH_2Leu), 51.6 (O-CH_3), 51.9 (αCH Leu), 60.0 (CH_2, N^{α}-Bn), 60.2 (αCH Ala), 79.7 (C, Boc), 127.6 (CH, Ar.), 128.2 (2 CH, Ar.), 128.8 (2 CH, Ar.), 136.4 (C, Ar.), 155.5 (C=O, Boc), 171.4 (C=O, hydrazid), 174.5 (C=O, ester); HRMS (ESI) calculated for $C_{22}H_{35}N_3O_5$ $[M+H]^+$ *m/z* 422.2655, found 422.2633 and 422.2638.

Pseudodipeptide Boc-[Glycine-*α*-N^{α}-benzyl-(D)-hydrazinoalanine]-OMe, 5. Amorphous solid. Characterization data: ^{1}H NMR (300 MHz, $CDCl_3$, 10 mM) δ 1.36-1.44 (m, 12H), 3.57-3.65 (m, 3H), 3.73 (s, 3H), 3.99-4.13 (m, 2H), 5.15 (br s, 1H), 7.26-7.39 (m, 5H), 7.56 (s, 1H); ^{13}C NMR (75 MHz, $CDCl_3$) δ 16.0 (CH_3), 28.2 (CH_3), 41.3 (CH_2), 51.7 (CH_3), 59.7 (CH), 61.9 (CH_2), 79.8 (C), 127.5 (CH), 127.8 (2 CH), 129.1 (2 CH), 136.1 (C), 155.5 (C=O), 172.3 (C=O), 174.2 (C=O); HRMS (ESI) calculated for $C_{18}H_{27}N_3O_5$ $[M+H]^+$ *m/z* 366.2023, found 366.1998.

HeterochiralpseudodipeptideBoc-[(L)-Leucine-α-N^{α}-benzyl-(D)-hydrazinoalanine]-NH_2,

6. White powder. Characterization data: mp 150°C; ^{1}H NMR (300 MHz, $CDCl_3$, 10 mM) δ 0.77 (d, 3H, J = 6.5 Hz), 0.80 (d, 3H, J = 6.5 Hz), 1.35 (d, 3H, J = 7.1 Hz), 1.45 (s, 9H), 1.40-1.62 (m, 3H), 3.51 (q, 1H, J = 7.1 Hz), 3.79-4.03 (m, 3H), 4.69 (br d, J = 7.5 Hz), 5.32 (s, 1H), 7.26-7.38 (m, 6H), 8.06 (br s). The physical data (NMR and HRMS) are in agreement with our values reported in Ref. 13.

ACKNOWLEDGMENTS

The authors acknowledge Dr Robert H. DODD for the critical reading of the manuscript, the DISCO Beamline in Synchrotron “Soleil” for giving us the opportunity to perform SRCD experiments, the FR3209 SCBIM Service Commun de Biophysique Interactions Moléculaires de l’Université de Lorraine for CD experiments and analysis, the experimental platform (Service Commun) of X-ray Diffraction of the Institut Jean Barriol for X-ray analysis and Mr Olivier Fabre for running NMR experiments.

SUPPORTING INFORMATION AVAILABLE

Copies of ^{1}H NMR, ^{13}C NMR spectroscopic data for compounds **1**-**5**. Concentration and solvent dependence ^{1}H NMR for compounds **2**-**4**. IR spectra and deconvolved IR spectra in $CDCl_3$ for compounds **2**-**4**.IR spectra in MeOH and Toluene for compounds **1**.Crystallographic data for compounds **1**-**4**. This material is available free of charge *via* the Internet at http://pubs.acs.org.

REFERENCES

(1) a) Taubes, G. *Science* **1996**, *271*, 1493; (b) Baumeister, R. ; Eimer, S. *Angew. Chem. Int. Ed*. **1998**, *37*, 2978.

(2) (a) Goedert, M.; Spillantini, M. G.; Davies, S. W. *Curr. Opin. Neurobiol.* **1998**, *8*, 619; (b) Spillantini, M. G.; Crowther, R. A.; Jakes, R.; Hasegawa, M.; Goedert, M. *Proc. Natl. Acad. Sci. USA* **1998**, *95*, 6469.

(3) Koo, E. H.; Lansbury, P. T., Jr; Kelly, J. W. *Proc. Natl. Acad. Sci. USA* **1999**, *96*, 9989.

(4) Cheguillaume, A.; Salaün, A.; Sinbandhit, S.; Potel, M.; Gall, P.; Baudy-Floc'h, M.; Le Grel, P. *J. Org. Chem.* **2001**, *66*, 4923.

(5) (a) Roy, O.; Faure, S.; Thery, V.; Didierjean, C.; Taillefumier, C.; *Org. Lett.* **2008**, *10*, 921; (b) Hjelmgaard, T.; Faure, S.; Caumes, C.; De Santis, E.; Edwards, A. A.; Taillefumier, C. *Org. Lett.* **2009**, *11*, 4100; (c) De Santis, E.; Hjelmgaard, T.; Faure, S.; Roy, O.; Didierjean, C.; Alexander, B. D.; Siligardi, G.; Hussain, R.; Javorfi, T.; Edwards, A. A.; Taillefumier, C. *AminoAcids***2011**, *41*, 663; (d) De Santis, E.; Hjelmgaard, T.; Caumes, C.; Faure, S.; Alexander, B. D.; Holder, S. J.; Siligardi, G.; Taillefumier, C.; Edwards, A. A. *Org. Biomol. Chem.* **2012**, *10*, 1108; (e) Caumes, C.; Fernandes, C.; Roy, O.; Hjelmgaard, T.; Wenger, E.; Didierjean, C.; Taillefumier, C.; Faure, S. *Org. Lett.* **2013**, *15*, 3626.

(6) (a) Seebach, D.; Ciceri, P. E.; Overhand, M.; Jaun, B.; Rigo, D.; Oberer, L.; Hommel, U.; Amstutz, R.; Widmer, H. *Helv. Chim. Acta***1996**, *79*, 2043; (b) Sifferlen, T.; Rueping, M.; Gademann, K.; Jaun, B.; Seebach, D. *Helv. Chim. Acta***1999**, *82*, 2067; (c) Abele, S.; Seebach, D. *Eur. J. Org. Chem.* **2000**, *1*, 1; (d) Gademann, K.; Ernst, M.; Seebach, D.; Hoyer, D. *Helv. Chim. Acta***2000**, *83*, 16 and references cited therein.

(7) (a) Appella, D. H.; Christianson, L. A.; Karle, I. L.; Powell, D. R.; Gellman, S. H. *J. Am. Chem. Soc.* **1996**, *118*, 13071; (b) Appella, D. H.; Christianson, L. A.; Klein, D. A.; Richards, M. R.; Powell, D. R.; Gellman, S.H. *J. Am. Chem. Soc.* **1999**, *121*, 7574; (c) Barchi, J. J., Jr; Huang, X.; Appella, D. H.; Christianson, L. A.; Durell, S. R.; Gellman, S. H. *J. Am. Chem. Soc.* **2000**, *122*, 2711; (d) Chung, Y. J.; Huck, B. R.; Christianson, L. A.; Stanger, H. E.; Krausthäuser, S.; Powell, D. R.; Gellman, S. H. *J. Am. Chem. Soc* .**2000**, *122*, 3995 and references cited therein.

(8) (a) Horne, W. S.; Stout, C. D.; Ghadiri, M. R. *J. Am. Chem. Soc.* **2003**, *125*, 9372; (b) Seebach, D.; Matthews, J. L.; Meden, A.; Wessels, T.; Baerlocher, C.; McCusker, L. B. *Helv. Chim. Acta***1997**, *80*, 173.

(9) (a) Pilsl, L. K. A.; Reiser, O. *Amino Acids* **2011**, *41*, 709; (b) Sharma, G. V. M.; Chandramouli, N.; Choudhary, M.; Nagendar, P.; Ramakrishna, K. V. S.; Kunwar, A. C.; Schramm, P.; Hofmann, H.-J. *J. Am. Chem. Soc.* **2009**, *131*, 17335; (c) Horne, W. S.; Gellman, S. H. *Acc. Chem. Res.* **2008**, *41*, 1399; (d) Roy, A.; Prabhakaran, P.; Baruah, P. K.; Sanjayan, G. J. *Chem. Commun.* **2011**, *47*, 11593; (d) Vasudev, P. G.; Chatterjee, S.; Shamala, N.; Balaram, P. *Acc. Chem. Res.* **2009**, *42*, 1628.

(10) (a) Guo, L.; Almeida, A. M.; Zhang, W.; Reidenbach, A. G.; Choi, S. H.; Guzei, I. A.; Gellman, S. H. *J. Am. Chem. Soc.* **2010**, *132*, 7868; (b) Karle, I. L.; Pramanik, A.; Banerjee, A.; Bhattacharjya, S.; Balaram, P. *J. Am. Chem. Soc.* **1997**, *119*, 9087; (c) Sharma, G. V. M.; Babu, B. S.; Ramakrishna, K. V. S.; Nagendar, P.; Kunwar, A. C.; Schramm, P.; Baldauf, C.; Hofmann, H.-J. *Chem. Eur. J.* **2009**, 15, 5552.

(11) (a) Steer, D. L.; Lew, R. A.; Perlmutter, P.; Smith, A. I.; Aguilar, M.-I. *Curr. Med. Chem.* **2002**, *9*, 811; (b) Guichard, G.; Zerbib, A.; Le Gal, F. A.; Hoebeke, J.; Connan, F.; Choppin, J.; Briand, J. P.; Guillet, J. G. *J. Med. Chem.* **2000**, *43*, 3803.

(12) Marraud, M.; Vanderesse, R. *R. in Houben-Weyl: Methods of Organic Chemistry, Vol. E22c* (Eds. Goodman, M.; Felix, A.; Moroder, L.; Toniolo, C.), Thieme: Stuttgart, New York, **2003**, pp 423-457.

(13) Moussodia, R.-O.; Acherar, S.; Bordessa, A.; Vanderesse, R.; Jamart-Grégoire, B. *Tetrahedron* **2012**, *68*, 4682.

(14) Moussodia, R.-O.; Acherar, S.; Romero, E.; Didierjean, C.; Jamart-Grégoire, B. *J. Org. Chem.* **2015**, *80*, 3022.

(15) (a) Koh, J. T.; Cornish, V. W.; Schultz, P. G. *Biochemistry* **1997**, *36*, 11314; (b) Chapman, E.; Thorson, J. S.; Schultz, P. G. *J. Am. Chem. Soc.* **1997**, *119*, 7151; (c) Shin, I.; Ting, A. Y.; Schultz, P. G. *J. Am. Chem. Soc.* **1997**, *119*, 12667; (d) Deechongkit, S.; Dawson, P. E.; Kelly, J. W. *J. Am. Chem. Soc.* **2004**, *126*, 16762.

(16) Lecoq, A.; Marraud, M.; Aubry, A. *Tetrahedron Lett.* **1991**, *32*, 2765.

(17) (a) Pispisa, B.; Stella, L.; Venanzi, M.; Palleschi, A.; Polese, A.; Formaggio, F.; Toniolo, C.*J. Peptide Res.* **2000**, *56*, 298; (b) Roy, R. S.; Karle, I. L.; Raghothama, S.; Balaram, P. *Proc. Natl. Acad. Sci. USA* **2004**, *101*, 16478; (c) Rai, R.; Raghothama, S.; Balaram, P. *J. Am. Chem. Soc.* **2006**, *128*, 2675; (d) Chang, X.-W.; Han, Q.-C.; Jiao, Z.-G.; Weng, L.-H.; Zhang, D.W. *Tetrahedron* **2010**, *66*, 9733; (e)Donoli, A.; Marcuzzo, V.; Moretto, A.; Crisma, M.; Toniolo, C.; Cardena, R.; Bisello, A.; Santi, S. *J. Biopolymers* **2013**, *100*, 14; (f)Acherar, S.; Salaün, A.; Le Grel, P.; Le Grel, B.; Jamart-Grégoire, B. *Eur. J. Org. Chem.* **2013**, 5603.

(18) Formaggio, F.; Crisma, M.; Toniolo, C.; Broxterman, Q. B.; Kaptein, B.; Corbier, C.; Saviano, M.; Palladino, P.; Benedetti, E. *Macromolecules* **2003**, *36*, 8164.

(19) For example see: Jacobsen, O, Gebreslasie, H. G.; Klaveness, J.; Rongved, P.; Görbitz, C. H. *Acta Crystallogr.* **2011,** *C67*, o278 and the references mentioned therein.

(20) Oku, H.; Yamada, K.; Katakai, R. *Biopolymers* **2008**, *89*, 270.

(21) Formaggio, F.; Moretto, A.; Crisma, M.; Toniolo, C. in *Peptide Materials from Nanostructures to Applications, Chap 2* (Eds.: Alemán, C.; Bianco, A.; Venanzi, M.), John Wiley & Sons, **2013**, pp 39-63.

(22) Wen, L.-R; Liu, P.; Li, M. *Acta Crystallogr.* **2007**, 63, o1212.

(23) (a) Castiglioni, E.; Biscarini, P.; Abbate, S. *Chirality* **2009**, *21*, E28; (b) Kuroda, R.; Harada, T. in *Comprehensive Chiroptical Spectroscopy, Instrumentation, Methodologies, and Theoretical Simulations, Chap. 4* (Eds.: Berova, N.; Polavarapu, P. L.; Nakanishi, K.; Woody, R. W.), John Wiley & Sons, Inc., **2012**,pp. 91-113.

(24) Greenfield, N.; Fasman, G. D.*Biochemistry* **1969**, *8*, 4108.

(25) Pescitelli, G.; Di Pietro, S.; Cardellicchio, C.; Capozzi, M. A. M.; Di Bari, L. *J. Org. Chem.* **2010**, *75*, 1143.

(26) (a) Le Grel, P.; Salaün, A.; Mocquet, C.; Le Grel, B.; Roisnel, T.; Potel, M. *J. Org. Chem.* **2011**, *76 (21)*, 8756; (b) Acherar, S.; Salaün, A.; Le Grel, B.; Jamart-Grégoire, B. *Eur. J. Org. Chem.* **2013**, 5603.

(27) (a) Schrauber, H.; Eisenhaber, F.; Argos, P. *J. Mol. Biol.* **1993**, *230*, 592; (b) MacKenzie, K. R.; Prestgard, J. H.; Engelman, D. M. *J. Biomol. NMR* **1996**, *7*, 256.

(28) Hariu, N.; Ito, M.; Akitsu, T. *Contemp. Eng. Sci.* **2015**, *8*, 57.

(29) (a) Kuroda, R. in *Circular Dichroism: Principles and Applications Second Edition* (Eds.: Berova, N.; Nakanishi, K.; Woody, R. W.), John Wiley & Sons, **2000**, pp 159-184; (b) Kuroda, R. Ph.D. Thesis, University of Tokyo, 1975.

(30) (a) *Comprehensive Chiroptical Spectroscopy, Applications in Stereochemical Analysis of Synthetic Compounds, Natural Products, and Biomolecules* (Eds.: Berova, N.; Prasad, L.; Polavarapu; Nakanishi, K.; Woody, R. W.), John Wiley& Sons, **2012**; (b) Kuroda, R.; Harada, T.; Shindo, Y. *Rev. Sci. Instrum*. **2001**, *72*, 3802; (c) Pescitelli, G.; Kurtán, T.; Flörke, U.; Krohn, K. *Chirality* **2009**, *21*, E181.

(31) Burla, M. C.; Caliandro, R.; Carrozzini, B.; Cascarano, G. L.; Cuocci, C.; Giacovazzo, C.; Mallamo, M.; Mazzone, Polidori, G. *J. Appl. Cryst.* **2015**, *48*, 306.

(32) Hübschle, C. B.; Sheldrick, G. M.; Dittrich, B. *J. Appl. Cryst.* **2011**, *44*, 1281.